Criticality of environmental information obtainable by dynamically controlled quantum probes

Analia Zwick,[1,2,3,4] Gonzalo A. Álvarez,[1,2] and Gershon Kurizki[1]
[1]*Weizmann Institute of Science, Rehovot 76100, Israel*
[2]*Centro Atómico Bariloche, CNEA, CONICET, 8400 S. C. de Bariloche, Argentina*
[3]*Instituto de Física Enrique Gaviola, CONICET, X5016LAE Córdoba, Argentina*
[4]*Facultad de Matemática, Astronomía y Física, Universidad Nacional de Córdoba, X5016LAE Córdoba, Argentina*
(Received 6 September 2015; revised manuscript received 16 August 2016; published 21 October 2016)

A universal approach to decoherence control combined with quantum estimation theory reveals a critical behavior, akin to a phase transition, of the information obtainable by a qubit probe concerning the memory time of environmental fluctuations of generalized Ornstein-Uhlenbeck processes. The criticality is intrinsic to the environmental fluctuations but emerges only when the probe is subject to suitable dynamical control aimed at inferring the memory time. A sharp transition is anticipated between two dynamical phases characterized by either a short or long memory time compared to the probing time. This phase transition of the environmental information is a fundamental feature that characterizes open quantum-system dynamics and is important for attaining the highest estimation precision of the environment memory time under experimental limitations.

DOI: 10.1103/PhysRevA.94.042122

I. INTRODUCTION

A quantum probe, such as a qubit, is capable of extracting information on the environment dynamics and its space-time fluctuations through the spectrum of the dephasing noise the probe is subjected to [1–14]. This information is the subject of an emerging field of research dubbed environmental quantum-noise spectroscopy [5,6]. Its most straightforward implementation is by monitoring the free-induction decay (FID) of an initially prepared qubit-probe coherence and inferring the dephasing characteristics from this decay [15–17]. A more promising option is to exert control (driving) fields, whether pulsed or continuous wave (CW), on the qubit probe and study its dephasing as a function of the control-field characteristics [4–6,18]. Pulsed control of qubit dephasing is commonly described by dynamical decoupling [19–23]. However, for the purpose of environment-noise spectroscopy it is useful to resort to the universal formula for the rate of decoherence under dynamical control [24–27], which is at the heart of the unified theory of dynamically controlled open quantum-systems [28–30]. This formula allows design of control fields or pulse-sequences that through the choice of a spectral filter function are optimally tailored to specific environment-noise spectrums and the task at hand [27,31]: decoherence control [24,25,28,29,32–36], state transfer [37,38], or storage [38–40] in a fluctuating environment. Here, the filter function will be adapted to the task of probing parameters of the environment-noise spectrum by a qubit [8,41].

Among environment parameters whose estimation is of practical interest in physics, chemistry, and biology, the *memory or correlation time* is particularly helpful [4–8,41–53]. On a fundamental level, environment memory effects are associated with the concept of non-Markovianity, whose definition is an outstanding issue [54,55].

For the purpose of characterizing memory effects of an environment that interacts with a qubit probe, we here put forward an approach based on the aforementioned universal formula for decoherence control [24–31] combined with quantum estimation theory [41,56–60]. We show that the information (estimation precision) concerning the environment-noise fluctuation spectrum obtained by this approach may exhibit *critical behavior* as a function of the memory-time parameter. This critical behavior, akin to a phase transition, is intrinsic to the environmental noise spectrum and is only revealed under dynamical control: it defines a *sharp boundary* between the short- and long-time regimes of the probe decoherence corresponding to long and short memory of the environment, respectively. By contrast, the FID of the probe coherence undergoes the usual *smooth transition* between the two dynamical regimes, thus conforming to the gradual change from non-Markovianity to Markovianity that has been previously analyzed [54,55]. The criticality or phase transition of the environmental information revealed here is a fundamental feature that serves as a means of characterizing dynamical behavior. Moreover, it is important for attaining the highest estimation precision of the environment memory time under experimental limitations.

II. CONTROLLED QUBIT PROBE AS A SENSOR OF THE ENVIRONMENTAL FLUCTUATIONS

We consider a *dynamically controlled* qubit probe experiencing pure dephasing due to the probe-environment interaction $H_{SB} = g\sigma_z B$, where σ_z is the Pauli operator for the probe and B is the environment operator. In the *weak-coupling probe-environment regime* [Fig. 1(a)], its dephasing is characterized by the attenuation (decay) factor $\mathcal{J}(\vec{x}_B,t)$ of the qubit coherence (Appendix A)

$$\langle\sigma_x(t)\rangle = \sigma_x(0)e^{-\mathcal{J}(\vec{x}_B,t)}, \tag{1}$$

where $\vec{x}_B$ is a set of parameters describing the environment and $\mathcal{J}(\vec{x}_B,t)$ obeys the universal formula [24–31]

$$\mathcal{J}(\vec{x}_B,t) = \int_{-\infty}^{\infty} d\omega\, F_t(\omega)G(\vec{x}_B,\omega). \tag{2}$$

Here $G(\vec{x}_B,\omega)$ is the coupling spectrum (spectral density) of the environment noise (the Fourier transform of its autocorrelation function). Explicitly, $\vec{x}_B = [g,\tau_c,\beta]$, with τ_c as the correlation or memory time of the environment noise, i.e., the inverse width of its spectral density, g as the

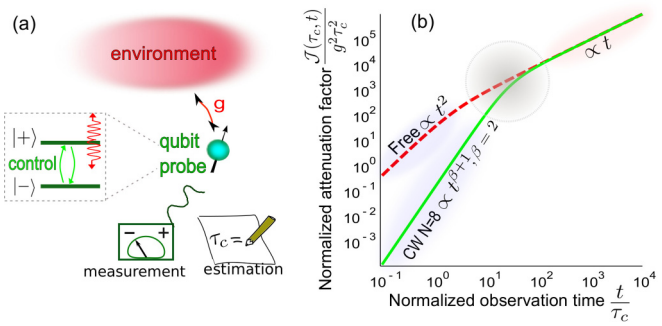

FIG. 1. (a) Estimation of the noise fluctuations by a qubit probing the environment. A dynamically controlled qubit probe undergoes pure dephasing due to the probe-environment interaction $H_{SB} = g\sigma_z B$. The dephasing is characterized on the qubit observable $\langle\sigma_x(\tau_c,t)\rangle \propto e^{-\mathcal{J}(\tau_c,t)}$ for an (optimal) initial-state: the symmetric superposition of the spin-up/-down states in the basis σ_z, $\frac{1}{\sqrt{2}}(|\uparrow\rangle + |\downarrow\rangle) = |+\rangle$ [59] (Appendix A). Here we focus in estimating τ_c. (b) Time dependence of the normalized attenuation factor $\mathcal{J}$ of the qubit state probing an Ornstein-Uhlenbeck process ($\beta = 2$) for free evolution (dashed) compared to its counterpart under dynamical control (solid). The latter time dependence exhibits a smooth transition (marked by a circle) between two well-defined dynamical phases (regimes) associated with a long and short memory time of the environment depending on the ratio $\frac{t}{\tau_c}$.

effective probe-environment coupling strength, and β as a power-law exponent that defines the type of stochastic (noise) process. The filter function $F_t(\omega)$ explicitly depends upon the dynamical control of the probe during time t. The information about the unknown environment parameters $\vec{x}_B$ is encoded by the probabilities p of finding the qubit probe in the $|+\rangle = \frac{1}{\sqrt{2}}(|\uparrow\rangle + |\downarrow\rangle)$ (symmetric) or $|-\rangle = \frac{1}{\sqrt{2}}(|\uparrow\rangle - |\downarrow\rangle)$ (antisymmetric) superposition of the qubit energy states when measuring σ_x. These probabilities obey

$$p_{\pm}(\vec{x}_B,t) = \tfrac{1}{2}(1 \pm e^{-\mathcal{J}(\vec{x}_B,t)}). \tag{3}$$

As a model to describe the memory time scales of the environment, we consider a *generalized Ornstein-Uhlenbeck spectral density*

$$G_\beta([g,\tau_c,\beta],\omega) = g^2 \frac{\mathcal{A}_\beta \tau_c}{1+\omega^\beta \tau_c^\beta}, \tag{4}$$

where $\mathcal{A}_\beta$ is a normalization factor depending on the power law $\beta \geqslant 2$. These types of bath spectra are ubiquitous in solid-state, liquid, or gas phases [5,8,41,47,61–64], where they are associated with collisional or diffusion processes: e.g., molecular diffusion in biological systems [8,42,43], charge diffusion in conducting crystals [44], or spin diffusion in complex spin networks [5,45–47]. This model is also a building block of universal lineshapes: it may characterize the memory-time of arbitrary bosonic baths, by assuming that a chosen harmonic-oscillator mode constitutes an interface between the qubit probe and the environment's modes [65]. The combined spectrum of any environment plus the interface mode is reshaped, or "filtered," according to the chosen oscillator-mode frequency and its coupling strength with the probe, resulting in a *skewed-Lorentzian lineshape* [65,66].

The power-law regime $\propto\omega^{-\beta}$ of the spectral density, obtained for $\omega\tau_c \gg 1$, is the spectral range with the strongest dependence on the frequency ω, describing the short-time behavior of the probe-qubit dephasing. We define this limit as the long-memory (LM) regime. In the opposite limit $\omega\tau_c \ll 1$, associated with long times, the spectral density becomes independent of the frequency, and the attenuation factor $\mathcal{J}(\vec{x}_B,t)$ is given by the Fermi golden rule. We dub this limit the short-memory (SM) regime.

III. IDENTIFYING THE DYNAMICAL REGIMES' CRITICALITY BY DYNAMICALLY CONTROLLED PROBES

Under FID, the LM and SM dynamical regimes are attained at times $t \ll \tau_c$ and $t \gg \tau_c$, respectively. The respective attenuation (decay) factors are $\mathcal{J}_{\rm free}^{LM} \propto g^2 t^2$ (independent of τ_c) and $\mathcal{J}_{\rm free}^{SM} \propto g^2\tau_c t$ (Appendix B 1). The transition from the LM to the SM regime is smooth [Fig. 1(b)] as the ratio $\frac{t}{\tau_c}$ is varied and does not depend on g. Invariably, $\frac{\partial \mathcal{J}_{\rm free}}{\partial \tau_c} \geqslant 0$, *without* sign change.

Consider now the change that may arise in the character of this transition under dynamical control. An example is a decoupling control sequence of $N \gg 1$ equidistant π pulses (known as CPMG) [16,67,68]. The filter function $F_t(\omega)$ [4,24–31] then converges to a sum of delta functions (narrowband filters) centered at the harmonics of the inverse modulation period, $k\omega_{\rm ctrl} = k\pi N/t$ with $k = 1,2,3,\ldots$ [5,36]. Another suitable control is CW qubit driving, which has a single frequency component ($k=1$). Under such controls, the LM and SM dynamical regimes are attained for $\omega_{\rm ctrl}\tau_c \gg 1$ and $\omega_{\rm ctrl}\tau_c \ll 1$, respectively. The corresponding decay factors considering the dominant filter frequency component, $\mathcal{J} \propto F_t(\omega_{\rm ctrl})G(\omega_{\rm ctrl})$ in Eq. (2), are [Fig. 1(b)] $\mathcal{J}^{LM} \propto g^2 t/(\omega_{\rm ctrl}^\beta \tau_c^{\beta-1})$ and $\mathcal{J}^{SM} \propto g^2\tau_c t$, respectively (Appendix B 2). This reflects the effect of narrow-band filters $F_t(\omega_{\rm ctrl})$ that may be used to scan the spectral density $G(\omega)$ [4–6], upon varying the modulating frequency (pulse rate or Rabi frequency) $\omega_{\rm ctrl}$ of the control field, all the way from the frequency-independent regime $G \propto \tau_c$ for $\omega\tau_c \ll 1$ to the power-law regime $G \propto \omega^{-\beta}\tau_c^{-(\beta-1)}$ for $\omega\tau_c \gg 1$ [Fig. 2(a)]. In the limit of extremely narrow spectral filters, i.e., $N \to \infty$, with $\omega_{\rm ctrl} = \pi N/t$, we have

$$\left.\frac{\partial \mathcal{J}}{\partial \tau_c}\right|_{\omega_{\rm ctrl}\sim\omega_0} \propto \left.\frac{\partial G}{\partial \tau_c}\right|_{\omega_{\rm ctrl}\sim\omega_0} \propto \omega_{\rm ctrl} - \omega_0. \tag{5}$$

Here $\omega_0 = \tau_c^{-1}(\beta-1)^{-\frac{1}{\beta}}$ is the probing frequency at which the dephasing rate is maximal for a given τ_c under the assumption of a narrow-band filter (Appendix C).

An abrupt change [Fig. 2(a)] is then revealed in the parametric sensitivity of the attenuation factor, defined by the derivative $\frac{\partial \mathcal{J}}{\partial \tau_c}$, through its *change of sign*: $\frac{\partial \mathcal{J}}{\partial \tau_c} \propto -(\beta-1)\tau_c^{-1}\mathcal{J}^{LM} < 0$ for LM and $\frac{\partial \mathcal{J}}{\partial \tau_c} \propto \tau_c^{-1}\mathcal{J}^{SM} > 0$ for SM, implying that (Appendix C)

$$\left.\frac{\partial \mathcal{J}}{\partial \tau_c}\right|_{\omega_{\rm ctrl}\approx\omega_0} = 0, \tag{6}$$

at a value dependent on the control frequency, when $\omega_{\rm ctrl} \approx \omega_0$.

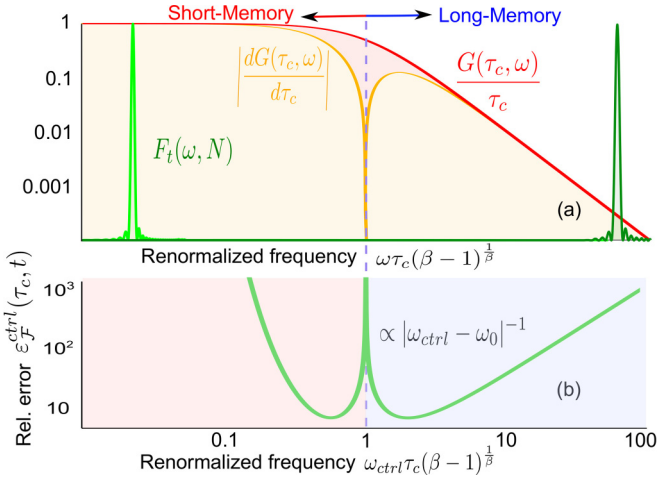

FIG. 2. Criticality of the probe-extracted information on the environmental correlation (memory) time τ_c. (a) Spectral density for the Ornstein-Uhlenbeck process (Lorentzian spectrum, $\beta = 2$: red solid-line). The spectrum's derivative $|\frac{dG}{d\tau_c}|$ exhibits a critical behavior $|\frac{dG}{d\tau_c}| \propto |\omega-\omega_0|$ at $\omega_0 = \tau_c^{-1}(\beta-1)^{-\frac{1}{\beta}}$ (orange, lighter solid-line). Then the two dynamical regimes occur when the narrow filters probe frequency components of $G(\omega)$ on both sides of the critical point. Two typical CW filter functions $F_t(\omega)$ (green sinc function curves, in linear scale) scan the spectrum on both sides of the transition ($N = 20$). (b) The attainable relative-error $\varepsilon_{\mathcal{F}}^{\rm ctrl}(\tau_c, t = \frac{\pi N}{\omega_{\rm ctrl}})$ on τ_c by the qubit probe under CW control ($\sqrt{2N}g\tau_c = 1$, $\beta = 2$, and $\omega_{\rm ctrl} = \frac{\pi N}{t}$, see Appendices B 2–E). The divergence $\propto |\omega_{\rm ctrl}-\omega_0|^{-1}$ at the critical point evidences the critical behavior of $|\frac{dG}{d\tau_c}|$.

Equation (6) signifies the vanishing of the quantum Fisher information (QFI) [56,57], which quantifies the attainable amount of information on τ_c that can be extracted from the measured probe (qubit) state probabilities $p_\pm$ under the specified control. This vanishing becomes apparent upon considering the expression for QFI [69] (Appendix D),

$$\mathcal{F}_{\mathcal{Q}}(\tau_c,t) = \frac{e^{-2\mathcal{J}}}{1-e^{-2\mathcal{J}}}\left(\frac{\partial\mathcal{J}}{\partial\tau_c}\right)^2. \tag{7}$$

Hence, at the finite value $\omega_{\rm ctrl} \approx \omega_0$ no information can be extracted on τ_c, $\mathcal{F}_{\mathcal{Q}}{}^{\rm ctrl}(\tau_c) = 0$. Since the minimum achievable relative error (per measurement) of the (unbiased) estimation of τ_c is related to the QFI through the Cramer-Rao bound as [56,57,70] (Appendix E),

$$\frac{\delta\tau_c}{\tau_c} \geqslant \varepsilon_{\mathcal{F}}(\tau_c,t) = \frac{1}{\tau_c\sqrt{\mathcal{F}_{\mathcal{Q}}(\tau_c,t)}}, \tag{8}$$

this error *diverges* as $\omega_{\rm ctrl} \to \omega_0$:

$$\varepsilon_{\mathcal{F}}^{\rm ctrl}\left(\tau_c, t \approx \frac{\pi N}{\omega_{\rm ctrl}}\right) \propto |\omega_{\rm ctrl}-\omega_0|^{-1}. \tag{9}$$

A central result of this paper is that the relative error in the estimation of τ_c, $\varepsilon_{\mathcal{F}}^{\rm ctrl}$, exhibits a *critical behavior* and a *sharp* transition between the LM and SM dynamical regimes [Fig. 2(b)], *witnessed through the vanishing of the QFI* at the finite control frequency $\omega_{\rm ctrl} \approx \omega_0$. This behavior allows their clear distinction. This *critical behavior* of the relative error provides a signature of*the environmental noise spectral density* through the values of τ_c and β, *provided we apply an appropriate dynamical control* that generates a sufficiently narrow spectral filter, so as to scan and witness the sign change of $\frac{\partial G}{\partial\tau_c}|_{\omega\sim\omega_0}$ at the critical point (Fig. 2). This manifested criticality is therefore intrinsic to the noise spectrum $G(\omega)$. By contrast, such criticality does not arise under FID, for which the filter function, $F_t^{\rm free}(\omega)$ is a much broader sinc function centered around $\omega = 0$ (Appendix A 1). The critical point divides the noise spectrum into distinct regimes of dephasing dynamics. This feature can serves as a means of characterizing the noise environment. Any spectral density of the noise that gives rise to a change of sign of $\frac{\partial\mathcal{J}}{\partial\tau_c}$ for a finite value of $\omega_{\rm ctrl}$, thus implying Eq. (6), will exhibit critical behavior.

IV. CRITICAL BEHAVIOR OF THE MAXIMAL ESTIMATION PRECISION OF τ_c

Another central result in this paper, with practical implications, is that the critical behavior shown above is also manifest, under the same control on the probe, for the *maximized estimation precision*, i.e., the smallest possible minimal relative error in the estimation of τ_c in Eq. (8),

$$\varepsilon_{\mathcal{F}}^{\rm ctrl}(\tau_c,t_{\rm opt}) = \min_t \varepsilon_{\mathcal{F}}^{\rm ctrl}(\tau_c,t). \tag{10}$$

The error minimization is the outcome of selecting the *optimal time* $t_{\rm opt}$ at which the measurement [cf. Eqs. (1) and (2)] is performed on the probe, following its dephasing under the control we have applied.

Figure 3 shows the critical behavior of the maximum precision per measurement, $\varepsilon_{\mathcal{F}}^{\rm ctrl}(\tau_c,t_{\rm opt})$, for the Lorentzian spectrum ($\beta = 2$) following CW control of the qubit probe as a function of $\sqrt{2N}g\tau_c$ (Appendices D and E).

The critical point

$$\sqrt{2N}g\tau_c \approx 1 \tag{11}$$

separates *two regions characterized by different scaling laws of the minimal relative error as a function of* $\sqrt{2N}g\tau_c$ [Fig. 3(a)]. These scaling laws are dictated by the different *dynamical regimes* for the attenuation-factor shown in Figs. 3(c) and 3(d).

The optimal probing (measurement) and control time $t_{\rm opt}$ also undergoes a sudden transition at the critical point (11), as shown in Fig. 3(b). This optimal time corresponds to the best tradeoff between a signal amplitude contrast, $e^{-2\mathcal{J}}/(1-e^{-2\mathcal{J}})$, and the parametric sensitivity of the signal attenuationfactor, $(\frac{\partial\mathcal{J}}{\partial\tau_c})^2$. The optimal tradeoff occurs [Fig. 3(b)] at either a long time compared to τ_c, $t_{\rm opt}^{SM}$ (red circle), corresponding to a linear attenuation factor $\mathcal{J}^{SM} \propto t$ [Fig. 3(c)], or at a short-time, $t_{\rm opt}^{LM}$ (blue circle), corresponding to $\mathcal{J}^{LM} \propto t^{\beta+1}$ [Figs. 3(d)]. These optimal control times in the two regimes are situated on both sides of the critical value [Fig. 3(b)], $t_{\rm opt}^{LM} < t_0 < t_{\rm opt}^{SM}$, $t_0 = \frac{\pi N}{\omega_0}$.

The criticality of the relative error as a function of $\omega_{\rm ctrl}$ described by Eq. (9) defines *two local,* unequal minimum values of $\varepsilon_{\mathcal{F}}^{\rm ctrl}$, located on either side of the critical point [Fig. 2(b) and insets of Fig. 3(a)]. What determines the *global* minima of $\varepsilon_{\mathcal{F}}^{\rm ctrl}$ is the optimal time $t_{\rm opt}$ obtained from Eq. (10). The critical behavior emerges when this global minimum *jumps* between the two local minima as a function of the parameter $\sqrt{2N}g\tau_c$ [Fig. 3(b)], resembling the behavior of

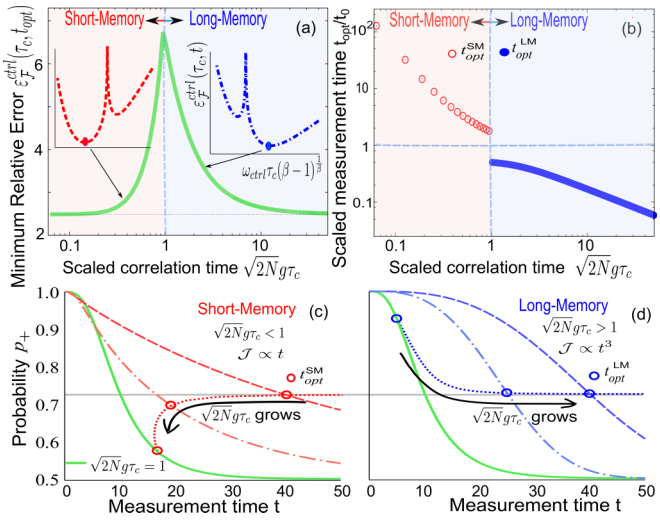

FIG. 3. Critical transition of the minimal error in the environment memory-time estimation determined by a probe under CW control in the narrow-filter approximation. The noise spectrum is a Lorentzian ($\beta = 2$). (a) The minimum relative error per measurement $\varepsilon_{\mathcal{F}}^{\rm ctrl}(\tau_c, t_{\rm opt})$ of the memory time τ_c, as a function of $\sqrt{2N}g\tau_c$, obtained by optimizing the control time $t_{\rm opt}$. It exhibits a critical behavior at $\sqrt{2N}g\tau_c \approx 1$. Insets: $\varepsilon_{\mathcal{F}}^{\rm ctrl}(\tau_c, t = \frac{\pi N}{\omega_{\rm ctrl}})$ for global minima located in the SM (left inset) and LM (right inset) regimes. The critical point emerges when both local minima are equal [as in Fig. 2(b)]. (b) The optimal scaled measurement time $\frac{t_{\rm opt}}{t_0}$ as a function of $\sqrt{2N}g\tau_c$. (c),(d) Probability $p_+(t)$ as a function of time. For $\sqrt{2N}g\tau_c < 1$, the optimal time $t_{\rm opt}^{SM}$ (red circles) corresponds to a linear attenuation factor $\mathcal{J}^{SM} \propto t$ [panel (c) and Fig. 1(b)], while for $\sqrt{2N}g\tau_c > 1$ the optimal time $t_{\rm opt}^{LM}$ (blue solid circles) belongs to a regime where $\mathcal{J}^{LM} \propto t^{\beta+1}$ [panel (d)]. At $\sqrt{2N}g\tau_c \approx 1$ [vertical dashed line in (a) and (b), green solid line in (c) and (d)] the transition between the two regimes is observed. The optimal time jumps between $t_{\rm opt}^{LM}$ and $t_{\rm opt}^{SM}$ at the critical point, avoiding the time $t_0 = \pi N \tau_c (\beta - 1)^{\frac{1}{\beta}}$ [horizontal dashed line in (b)] where no information about τ_c can be extracted from the probe.

conventional phase transitions. At the critical point, both local minima are equal, as displayed in Fig. 2(b), which leads to the fastest decay in the narrow-band limit as seen in Figs. 3(c) and (d) by the green solid line.

V. DISCUSSION

We demonstrated a critical behavior of information (estimation precision) on the environment fluctuation (noise) spectrum of a generalized Ornstein-Uhlenbeck process, extracted by a probe subject to appropriate dynamical control as a function of the ratio between the probing time and the environment memory time t/τ_c. This finding applies to any environment characterized by such spectra that are ubiquitous in solid-state, liquid, or gas phases [5,8,44–47,61–64].

We have shown that similar critical behavior is manifest for the maximal estimation precision of τ_c. At the critical point there is a massive loss of information on τ_c. Near this point, the optimal time for measuring and controlling the quantum probe is either very short, corresponding to little parametric

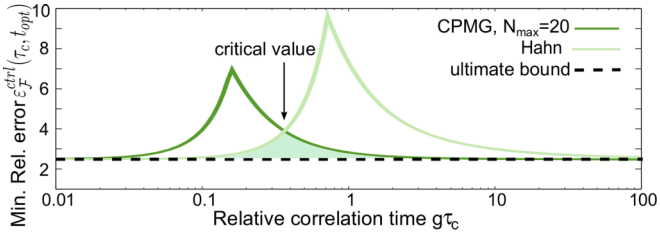

FIG. 4. Minimal relative error per measurement in the estimation of τ_c as a function of $g\tau_c$ for a Lorentzian environmental spectrum under dynamical control. Practical limitations on the number of pulses of a CPMG sequence, such that $N \leqslant N_{\rm max}$, may prevent attaining the ultimate bound (dashed line). A sudden change of the dynamical control strategy as a function of $g\tau_c$ may help: For $g\tau_c$ lower than the critical value, the highest precision is achieved by the single-pulse Hahn echo ($N = 1$). However, if $g\tau_c$ is larger than the critical value, the CPMG sequence with $N = N_{\rm max}$ is optimal. This dynamical control strategy under practical limitations reduces the minimal error represented by the shaded area, which is determined by the optimal control on each side of the intersection (critical value) of the Hahn and the CPMG curves.

sensitivity, or very long, corresponding to a significant decay of the probe signal.

The critical behavior of the maximal estimation precision of τ_c has paramount practical implications:

(i) Complete dynamical behavior characterization: Rather than mapping out the long- and short-memory probe dynamics regimes by varying the probing time, the critical behavior demonstrated here allows one to characterize the complete dynamics as consisting of *two* distinct *dynamical phases* (regimes) according to the maximal information they yield about the environment memory time. These two dynamical phases are sharply separated by the critical point (11).

(ii) Sudden change of the optimal dynamical control sequence: The critical point depends on the control scheme; thus, for CPMG control [16,67,68] $g\tau_c \approx 1/\sqrt{2N}$ when probing a Ornstein-Uhlenbeck process (Lorentzian spectra). This fact highlights the importance of optimizing the number of pulses N to improve the estimation precision, if N is bounded by $N_{\rm max}$ due to practical limitations on the power deposition and/or on the pulse length. Under these conditions, the *ultimate bound* on the estimation precision found in Ref. [41], $\varepsilon_{\mathcal{F}}(\tau_c, t) \geqslant \varepsilon_0 \approx 2.48$, may not be attained for $g\tau_c \lesssim 1/\sqrt{2N_{\rm max}}$. A sudden change of N should be undertaken as a function of $g\tau_c$ to optimize the estimation: For $g\tau_c$ lower than a certain critical value shown in Fig. 4, the best precision is achieved by the single-pulse Hahn echo ($N = 1$). However, if $g\tau_c$ is larger than this critical value, the CPMG sequence with $N = N_{\rm max}$ is optimal. Qualitatively similar considerations apply for generalized Ornstein-Uhlenbeck processes.

To sum up, the critical behavior of the environmental information revealed here is a fundamental feature that characterizes open quantum-system dynamics and is important for attaining the highest estimation precision of the environment memory time under practical limitations. It represents an alternative characterization of the probe-qubit dynamics under suitable control or observation that leads to a phase transition on the dynamical behavior [46,71–76]. Intriguingly,

the *absence of information* on τ_c has been shown to provide a distinctive signature of the environmental noise estimation.

Such information may be useful, e.g., for studying molecular diffusion at the nanoscale and thereby characterizing biological systems [8,41–43] or chemical-identities [7], charge diffusion in conducting crystals [44], or spin diffusion in complex spin networks [5,45–47,77]. Knowledge of the memory time may also be important for studying fundamental effects, such as quantum phase-transitions in a spin environment [48,49] or nonlocal correlations within a composite environment [50–53]. We envisage that this critical behavior may be exploited to characterize noises/baths with multiple memory-times as in the case of spectral densities described by sums of Lorentzians [42,63,78]. Multiple peaks of the relative-error associated with such a generalized memory-time may be revealed as a function of the control parameters that determine the shape of the appropriate filter-functions.

ACKNOWLEDGMENTS

We are grateful to Dieter Suter for fruitful discussions. G.K. acknowledges ISF support under the Bikura (Prime) grant. G.A.A. acknowledges the support of the European Commission under the Marie Curie Intra-European Fellowship for Career Development, Grant No. PIEF-GA-2012-328605. A.Z. and G.A.A. acknowledge the support of Consejo Nacional de Investigaciones Científicas y Técnicas (CONICET) and CNEA.

APPENDIX A: QUBIT PROBE UNDER DEPHASING

Here we provide the background necessary for Sec. II, "Controlled qubit probe as a sensor of the environmental fluctuations."

1. Weak coupling regime description

A single qubit probe (denoted here as system) experiences dephasing due to its interaction with the environment (bath) and undergoes control. They are described by the Hamiltonian

$$H = H_S(t) + H_B + H_{SB}, \tag{A1}$$

where S and B label the system and environment respectively, and

$$H_S = \omega_z \frac{(I+\sigma_z)}{2} + V_x(t)\sigma_x, \quad H_{SB} = S \otimes B = \sigma_z g B, \tag{A2}$$

$\sigma_{x,y,z}$ being the Pauli operators of the qubit, $(I+\sigma_z)/2 = |\uparrow\rangle\langle\uparrow|$ being $|\uparrow\rangle$ the upper (excited) state of the qubit probe, ω_z its resonant frequency, $V_x(t) = V(t)e^{-i\omega_z t} + \text{c.c.}$ the control acting on the qubit, and g the qubit-bath coupling strength. The actual form of the environment Hamitonian H_B can be in general arbitrary, and it is not relevant for the present discussion.

A *non-Markovian* master equation for the density matrix of the system $\rho_S(t)$ can be derived in the interaction picture. Under the Born approximation, also known as the weak-coupling regime, the system-environment coupling strength g is assumed to be weak enough for the influence of the system on the density matrix of the environment ρ_B to be negligible. As a result, the density matrix of the total system at a time t can be expressed as $\rho(t) \approx \rho_S(t) \otimes \rho_B$ [79], yielding the non-Markovian master equation [24–26,28,80]

$$\dot{\rho}_S(x_B,t) = \int_0^t dt' \{g^2 \Phi(x_B, t-t')[S(t'), S(t)\rho_S(t)] + \text{H.c}\}. \tag{A3}$$

Here $\Phi(x_B,t'-t'') = \text{Tr}_B\{B(t'-t'')B(0)\rho_B(0)\}$ is the environment autocorrelation function, x_B is a parameter that characterizes the environment, and, in the interaction picture,

$$\begin{aligned} S(t) &= U_S^\dagger(t) S U_S(t), \\ U_S(t) &= \mathcal{T} \exp\left(-i \int_0^t dt' H_S(t')\right), \\ B(t) &= U_B^\dagger(t) B U_B(t), \quad U_B(t) = e^{-iH_B t}. \end{aligned} \tag{A4}$$

2. The attenuation factor of the qubit-probe dephasing

The phase due to the unperturbed energy difference ω_z is irrelevant for describing the dephasing experienced by the qubit probe. This phase dependence can be eliminated by transforming to the rotating frame that can be described by the time-dependent basis

$$|p_\pm\rangle = \frac{1}{\sqrt{2}}(e^{-i\omega_z t}|\uparrow\rangle \pm |\downarrow\rangle), \tag{A5}$$

where $|\downarrow\rangle$ and $|\uparrow\rangle$ are the lower and upper states of the qubit probe in the laboratory frame, respectively. The system Hamiltonian of Eq. (A1) tilted in this basis becomes

$$\tilde{H}_S = \frac{V(t)}{2}\tilde{\sigma}_z, \quad \tilde{\sigma}_z = |p_+\rangle\langle p_+| - |p_-\rangle\langle p_-|, \tag{A6}$$

while H_B and H_{SB} remain invariant. We now go to the interaction picture as described in the previous section and write Eqs. (A4) as

$$\begin{aligned} U_S(t) &= \Omega_0(t)|p_+\rangle\langle p_+| + \Omega_0^*(t)|p_-\rangle\langle p_-|, \\ S(t) &= \Omega(t)|p_+\rangle\langle p_-| + \Omega^*(t)|p_-\rangle\langle p_+|, \end{aligned} \tag{A7}$$

where

$$\Omega_0(t) = \exp\left(-i\int_0^t \frac{V(t')}{2}dt\right), \tag{A8}$$

$$\Omega(t) = \exp\left(i\int_0^t V(t')dt\right) \tag{A9}$$

allows us to express the quantum master equation of Eq. (A3) as [24–26,28,80]

$$\frac{d}{dt}(\Delta\rho_{S,\pm}) = -\frac{d\mathcal{J}}{dt}\Delta\rho_{S,\pm}. \tag{A10}$$

Here $\Delta\rho_{S,\pm} = \rho_{S,++} - \rho_{S,--}$ represents the qubit-coherence in the basis $\{|\downarrow\rangle, |\uparrow\rangle\}$ at time t,

$$\langle\sigma_x(t)\rangle = \langle\tilde{\sigma}_z(t)\rangle = \Delta\rho_{S,\pm} = e^{-\mathcal{J}(x_B,t)}\langle\sigma_x(0)\rangle, \tag{A11}$$

which is characterized by the attenuation factor [24–26,28,80]

$$\mathcal{J}(x_B,t) = \text{Re}\left[\int_0^t dt' \int_0^{t'} dt'' g^2 \Phi(x_B, t'-t'')\Omega(t')\Omega^*(t'')\right]. \tag{A12}$$

In the spectral representation, this attenuation factor becomes

$$\mathcal{J}(x_B,t) = \int_{-\infty}^{\infty} d\omega\, F_t(\omega) G(x_B,\omega), \tag{A13}$$

where

$$G(x_B,\omega) = \frac{1}{2\pi}\int_{-\infty}^{\infty} dt\, g^2 \Phi(x_B,t) e^{i\omega t} \tag{A14}$$

is the *environment-coupling spectrum* given by the Fourier transform of the environmental-correlation function which is normalized in the frequency domain,

$$\int_{-\infty}^{\infty} d\omega\, G(x_B,\omega) = g^2, \tag{A15}$$

and

$$F_t(\omega) = \frac{1}{2\pi}\left|\int_0^t dt' \Omega(t') e^{i\omega t'}\right|^2 \tag{A16}$$

is the *control-field filter function*. It is determined by the finite-time Fourier transform of the dynamical control on the qubit probe which satisfies the following sum rule:

$$\int_{-\infty}^{\infty} \frac{d\omega}{\pi} F_t(\omega) = t. \tag{A17}$$

APPENDIX B: DEPHASING ATTENUATION FACTORS FOR GENERALIZED ORNSTEIN-UHLENBECK SPECTRA

In the following we derive the dephasing attenuation factor, Eq. (A13) with $x_B = \tau_c$, presented in Sec. III, "Identifying the dynamical regimes' criticality by dynamically controlled probes" of the main text, and plotted in Fig. 1(b). There, the qubit probe experiences dephasing due to the interaction with an environment, Eq. (A14), described by the generalized Ornstein-Uhlenbeck spectral density

$$G(\tau_c,\omega) = g^2 \frac{\mathcal{A}_\beta \tau_c}{1+\omega^\beta \tau_c^\beta} \tag{B1}$$

where $\mathcal{A}_\beta = \frac{\beta}{2\pi}\sin(\frac{\pi}{\beta})$ is a normalization factor in accordance with Eq. (A15). Here the actual form of H_B has to lead to an autocorrelation function $\Phi(x_B,t)$ whose Fourier transform, Eq. (A14), gives Eq. (B1). These types of bath spectra are ubiquitous in solid-state, liquid, or gas phases [5,8,41,47,61–64], where they are associated with collisional or diffusion processes, e.g., molecular diffusion in biological systems [8,42,43], charge diffusion in conducting crystals [44], or spin diffusion in complex spin networks [5,45–47].

1. Dephasing attenuation factor under free evolution of the quantum probe

The filter function (A16) for a freely evolving qubit probe over a total time t, the free-induction decay, is given by

$$F_t^{\text{free}}(\omega) = \frac{1}{2}\left|\frac{e^{-\frac{i\omega t}{2}}\sin\left(\frac{\omega t}{2}\right)}{\frac{\omega}{2}}\right|^2 = \frac{t^2}{2}\,\text{sinc}^2\left(\frac{\omega t}{2}\right). \tag{B2}$$

Then, we obtain the dephasing attenuation factor for a freely evolving qubit probe by introducing Eqs. (B1) and (B2) in Eq. (A13) and by considering the short-memory (SM) or long-memory (LM) regimes.

In the LM regime, i.e., $t \ll \tau_c$, the relevant part of the filter function (B2) becomes frequency independent,

$$F_t^{\text{free}} \approx \frac{t^2}{2}, \tag{B3}$$

leading, along with Eq. (A15), to the attenuation factor

$$\mathcal{J}_{\text{free}}^{SM}(\tau_c,t) \approx \int_{-\infty}^{\infty} d\omega \frac{t^2}{2} G(\tau_c,\omega) = \frac{1}{2} g^2 t^2. \tag{B4}$$

In the SM regime, i.e., $t \gg \tau_c$, the filter function from Eq. (B2) is a *narrow sinc function* centered at $\omega = 0$. There, the spectral density (B1) is well approximated as $G(\tau_c,\omega) \approx G(\tau_c,\omega=0)$, leading to an attenuation factor

$$\mathcal{J}_{\text{free}}^{SM}(\tau_c,t) \approx \int_{-\infty}^{\infty} d\omega\, F_t^{\text{free}}(\omega)\, G(\tau_c,\omega=0) = g^2 \pi \mathcal{A}_\beta \tau_c t, \tag{B5}$$

where we invoke the filter function property (A17).

2. Dephasing attenuation factor for dynamically controlled quantum probe under the narrow-band filter approximation

The filter functions (A16) for a dynamically controlled qubit probe under CPMG and Hahn (spin-echo) sequences or CW driving over a total time t are given respectively by [4,36]

$$F_t^{CPMG}(\omega,N) = \left|\frac{i2e^{-\frac{i\omega t}{2}}\sin^2\left(\frac{\omega t}{4N}\right)(e^{\frac{1}{2}i\omega t}+(-1)^{N+1}e^{-\frac{1}{2}i\omega t})}{\cos\left(\frac{\omega t}{2N}\right)\omega}\right|^2, \tag{B6}$$

for a CPMG sequence of N π pulses,

$$F_t^{\text{Hahn}}(\omega) = \left|\frac{ie^{-\frac{i\omega t}{2}}\sin^2\left(\frac{\omega t}{4}\right)}{\frac{\omega}{4}}\right|^2. \tag{B7}$$

for a Hahn sequence obtained by setting $N = 1$ in Eq. (B6) and

$$F_t^{CW}(\omega,N) = \frac{T^2}{2}[\text{sinc}^2(\nu_+) + \text{sinc}^2(\nu_-)], \quad \nu_\pm = \pi \text{N} \pm \omega \text{T}, \tag{B8}$$

for CW N-period driving.

The attenuation factor in Eq. (A13) for CPMG or CW dynamical controls acting on the qubit probe under the narrow-band filter approximation [5,36] is

$$\mathcal{J}(\tau_c,t) = \sum_{k=1}^{\infty} F_t(k\omega_{\text{ctrl}}) G(\tau_c,k\omega_{\text{ctrl}}), \tag{B9}$$

where $k\omega_{\text{ctrl}}$ are the harmonics of the CPMG or CW modulation functions. In keeping with the main text, here we consider the generalized Ornstein-Uhlenbeck spectra in Eq. (B1).

In the long-memory (LM) regime, where $\omega_{\text{ctrl}}\tau_c \gg 1$, $\omega_{\text{ctrl}} = \frac{t}{\pi N}$, the attenuation factor becomes

$$\mathcal{J}^{LM}(\tau_c,t) \approx g^2 \sum_{k=1}^{\infty} F_t\left(\frac{\pi k N \tau_c}{t}\right) \frac{\mathcal{A}_\beta \tau_c}{\left(\frac{\pi k N \tau_c}{t}\right)^\beta} = \frac{c_\beta g^2 t^{\beta+1}}{N^\beta \tau_c^{\beta-1}}, \tag{B10}$$

with

$$c_\beta = \frac{\beta}{2\pi^\beta} \sin\left(\frac{\pi}{\beta}\right) \tag{B11}$$

for CW control (only the first harmonic $k = 1$ is nonzero) and

$$c_\beta = \frac{\zeta(\beta+2)(4-2^{-\beta})\beta}{\pi^{2\beta}} \sin\left(\frac{\pi}{\beta}\right) \tag{B12}$$

for CPMG control (only odd k harmonics are nonzero), where ζ is the zeta function defined for $\mathrm{Re}(z) > 1$ as $\zeta(z) = \Sigma_{i=1}^{\infty} \frac{1}{i^z}$. It turns out that $c_\beta^{CW} \approx c_\beta^{CPMG}$.

In the short-memory (SM) regime, $\omega_{\mathrm{ctrl}}\tau_c \ll 1$, the attenuation factor is given by the Fermi golden rule (B5),

$$\mathcal{J}^{SM}(\tau_c,t) = g^2\pi\mathcal{A}_\beta\tau_c t, \tag{B13}$$

which holds for both CW and CPMG controls.

APPENDIX C: DERIVATIVE OF THE ATTENUATION FACTOR UNDER THE NARROW-BAND APPROXIMATION

Here we describe the maximum dephasing rate for a given τ_c discussed between Eqs. (5) and (6) in the main text.

The derivative of the attenuation factor, Eq. (A13), with respect to τ_c is

$$\frac{\partial\mathcal{J}(\tau_c,t)}{\partial\tau_c} = \int_{-\infty}^{\infty} d\omega\, F_t(\omega)\frac{\partial G(\tau_c,\omega)}{\partial\tau_c}. \tag{C1}$$

For a generalized Ornstein-Uhlenbeck spectral density, Eq. (B1), the argument of the integral has a zero $\frac{\partial G}{\partial\tau_c}|_{\omega=\omega_0} = 0$ at

$$\omega_0 = \frac{1}{\tau_c(\beta-1)^{\frac{1}{\beta}}}. \tag{C2}$$

Near this zero

$$\left.\frac{\partial G}{\partial\tau_c}\right|_{\omega\sim\omega_0} \propto \omega - \omega_0. \tag{C3}$$

Under the narrow-band filter approximation in Eq. (B9) provided by suitable CW control, Eq. (C1) becomes dependent on a single frequency $\omega_{\mathrm{ctrl}} = \frac{\pi N}{t}$. This implies that when $\omega_{\mathrm{ctrl}} \sim \omega_0$

$$\left.\frac{\partial\mathcal{J}}{\partial\tau_c}\right|_{\omega_{\mathrm{ctrl}}\sim\omega_0} \propto \left.\frac{\partial G}{\partial\tau_c}\right|_{\omega_{\mathrm{ctrl}}\sim\omega_0} \propto \omega_{\mathrm{ctrl}} - \omega_0 \tag{C4}$$

and

$$\left.\frac{\partial\mathcal{J}}{\partial\tau_c}\right|_{\omega_{\mathrm{ctrl}}\approx\omega_0} = 0. \tag{C5}$$

Remarkably, the zero in (C5) is *only observed under suitable control,* as we described. By contrast, a *freely evolving* qubit probe generates a filter function centered at frequency $\omega = 0$, Eq. (B2), that may overlap not only with ω_0 but also with the entire spectrum $|\omega| < \omega_0$, preventing us from distilling the contribution of ω_0 related to the criticality of the environmental information.

APPENDIX D: QUANTUM FISHER INFORMATION ON THE ENVIRONMENT MEMORY TIME

The quantum Fisher information on the environment memory time τ_c is extractable from the probe qubit state through the expression [41,56,57,59,69,81]

$$\mathcal{F}_Q = \frac{1}{p_+}\left(\frac{\partial p_+}{\partial\tau_c}\right)^2 + \frac{1}{p_-}\left(\frac{\partial p_-}{\partial\tau_c}\right)^2 + 2\frac{(p_+-p_-)^2}{p_++p_-} \times\left(\left|\langle p_-|\frac{\partial|p_+\rangle}{\partial\tau_c}\right|^2 + \left|\langle p_+|\frac{\partial|p_-\rangle}{\partial\tau_c}\right|^2\right), \tag{D1}$$

where

$$p_\pm(\tau_c,t) \equiv p(\pm|\tau_c,t) = \tfrac{1}{2}(1 \pm e^{-\mathcal{J}(\tau_c,t)}) \tag{D2}$$

are the respective probabilities of finding the qubit probe in the states $|\pm\rangle = \frac{1}{\sqrt{2}}(|\uparrow\rangle \pm |\downarrow\rangle)$, but also the eigenvalues of the qubit-probe density matrix in the $|p_\pm\rangle$ basis [Eq. (A5)] [28,80].

The measurement on the qubit probe that provides more information is effected by projections onto the eigenstates $|p_\pm\rangle$ of σ_x in the rotating frame. When the quantum Fisher information $\mathcal{F}_Q$ coincides with its classical counterpart, the measurement is said to be optimal [56,57,59,81]. This is the case here, under pure dephasing, when the last term in (D1) is null, given that $\frac{\partial|p_\pm\rangle}{\partial\tau_c} = 0$.

Then, Eq. (D1) becomes

$$\mathcal{F}_Q(\tau_c,t) = \frac{e^{-2\mathcal{J}(\tau_c,t)}}{1-e^{-2\mathcal{J}(\tau_c,t)}}\left(\frac{\partial\mathcal{J}(\tau_c,t)}{\partial\tau_c}\right)^2, \tag{D3}$$

for the optimal initial probe state $|+\rangle$. For an arbitrary initial state, $(\cos(\theta)|\uparrow\rangle + i\,\sin(\theta)|\downarrow\rangle), 0 < \theta < \frac{\pi}{2}$, $\mathcal{F}_Q(\tau_c,t) \propto \sin^2(2\theta)$ [59]. Under this condition the optimal initial state maximizes the quantum Fisher information when $\theta = \frac{\pi}{4}$.

APPENDIX E: ANALYTICAL ATTENUATION FACTORS FOR ORNSTEIN-UHLENBECK PROCESSES

Here we provide analytical expressions for the dephasing attenuation factor in Ornstein-Uhlenbeck processes [i.e., Lorentzian spectrum $\beta = 2$ in Eq. (B1)] supporting the numerical simulations presented in Figs. 1–4. Analytical expressions for the attenuation factors under CPMG [8] and CW control sequences can be derived in the form

$$\mathcal{J}_{CW}(\tau_c,t) = -\frac{g^2t^6}{\tau_c^3}\frac{\left(1+\frac{2\tau_c(-1)^N e^{-\frac{t}{\tau_c}}}{t} + \left(\frac{\tau_c N\pi}{t}\right)^2 - \frac{2\tau_c}{t}\right)}{\left(N^2\pi^2+\frac{t^2}{\tau_c^2}\right)^2} \tag{E1}$$

$$\mathcal{J}_{CPMG}(\tau_c,t) = -g^2\tau_c t^2\left[1-\frac{\tau_c}{t}\left(A_1(t) - 4\frac{A_2(t)+A_3(t)}{(e^{-\frac{t}{N\tau_c}}+1)^2}\right)\right], \tag{E2}$$

$$A_1(t) = (2N+1) - (-1)^N e^{-\frac{t}{\tau_c}},$$

$$A_2(t) = ((-1)^{N+1}e^{-\frac{t}{\tau_c}} + 1)(e^{-\frac{3}{2}\frac{t}{N\tau_c}} + e^{-\frac{1}{2}\frac{t}{N\tau_c}} - e^{-\frac{t}{N\tau_c}}),$$

$$A_3(t) = N(e^{-2\frac{t}{N\tau_c}} + e^{-\frac{t}{N\tau_c}}).$$

The CPMG sequence with a single pulse $N = 1$ is the well-known Hahn sequence. By evaluating $N = 1$ in Eq. (E2), we obtain the corresponding attenuation factor

$$\mathcal{J}_{\rm Hahn}(\tau_c,t) = -g^2\tau_c t\left[1 - \frac{\tau_c}{t}(3 + e^{-\frac{t}{\tau_c}} - 4e^{-\frac{t}{2\tau_c}})\right]. \quad \text{(E3)}$$

Upon inserting Eqs. (E1) and (E2) in Eq. (D3), we find an analytical expression for the quantum Fisher information concerning the memory time τ_c [Eq. (7) in the main text]. This allows us to analytically express the minimum relative error dictated by the Cramer-Rao bound [56,57,70], as per Eq. (8) in the main text,

$$\varepsilon_{\mathcal{F}}(\tau_c,t) = \frac{1}{\tau_c\sqrt{\mathcal{F}_Q(\tau_c,t)}} \quad \text{(E4)}$$

that was displayed in Fig. 2(b), and in the insets of Figs. 3(a) and 3(b).

The optimal times $t_{\rm opt}$ [displayed in Figs. 3(b)–3(d)] that globally minimize the minimum relative error $\varepsilon_{\mathcal{F}}(\tau_c,t_{\rm opt}) = \min_t \varepsilon_{\mathcal{F}}(\tau_c,t)$ [displayed in Figs. 3(a) and 4) were numerically obtained from the analytical expression of $\varepsilon_{\mathcal{F}}(\tau_c,t)$ using Eqs. (E1), (E2), and (D3).

A good approximation for the optimal time under CPMG control for the entire SM regime is

$$t_{\rm opt}^{SM} \approx \frac{W(-2e^{-2-4(N+\frac{1}{2})g^2\tau_c^2}) + 2 + (8N+4)g^2\tau_c^2}{2g^2\tau_c}, \quad \text{(E5)}$$

which corresponds to $\sqrt{2N}g\tau_c < 1$ in Figs. 3 and 4 in the main text.

For the LM regime

$$t_{\rm opt}^{LM} \approx \tau_c \sqrt[\beta+1]{\frac{N^\beta \mathcal{J}_0}{c_\beta g^2\tau_c^2}}, \quad \text{(E6)}$$

provided $\sqrt{2N}g\tau_c \gg 1$, under CPMG and CW controls.

[1] A. Mittermaier and L. Kay, Science **312**, 224 (2006).
[2] J. M. Taylor, P. Cappellaro, L. Childress, L. Jiang, D. Budker, P. R. Hemmer, A. Yacoby, R. Walsworth, and M. D. Lukin, Nat. Phys. **4**, 810 (2008).
[3] G. Balasubramanian, I. Y. Chan, R. Kolesov, M. Al-Hmoud, J. Tisler, C. Shin, C. Kim, A. Wojcik, P. R. Hemmer, A. Krueger, T. Hanke, A. Leitenstorfer, R. Bratschitsch, F. Jelezko, and J. Wrachtrup, Nature (London) **455**, 648 (2008).
[4] I. Almog, Y. Sagi, G. Gordon, G. Bensky, G. Kurizki, and N. Davidson, J. Phys. B: At. Mol. Opt. Phys. **44**, 154006 (2011).
[5] G. A. Álvarez and D. Suter, Phys. Rev. Lett. **107**, 230501 (2011).
[6] J. Bylander, S. Gustavsson, F. Yan, F. Yoshihara, K. Harrabi, G. Fitch, D. G. Cory, Y. Nakamura, J. Tsai, and W. D. Oliver, Nat. Phys. **7**, 565 (2011).
[7] P. E. S. Smith, G. Bensky, G. A. Álvarez, G. Kurizki, and L. Frydman, Proc. Natl. Acad. Sci. USA **109**, 5958 (2012).
[8] G. A. Álvarez, N. Shemesh, and L. Frydman, Phys. Rev. Lett. **111**, 080404 (2013).
[9] G. Kucsko, P. C. Maurer, N. Y. Yao, M. Kubo, H. J. Noh, P. K. Lo, H. Park, and M. D. Lukin, Nature (London) **500**, 54 (2013).
[10] P. Neumann, I. Jakobi, F. Dolde, C. Burk, R. Reuter, G. Waldherr, J. Honert, T. Wolf, A. Brunner, J. H. Shim, D. Suter, H. Sumiya, J. Isoya, and J. Wrachtrup, Nano Lett. **13**, 2738 (2013).
[11] D. M. Toyli, C. F. d. l. Casas, D. J. Christle, V. V. Dobrovitski, and D. D. Awschalom, Proc. Natl. Acad. Sci. USA **110**, 8417 (2013).
[12] S. Steinert, F. Ziem, L. T. Hall, A. Zappe, M. Schweikert, N. Götz, A. Aird, G. Balasubramanian, L. Hollenberg, and J. Wrachtrup, Nat. Commun. **4**, 1607 (2013).
[13] M. S. Grinolds, M. Warner, K. D. Greve, Y. Dovzhenko, L. Thiel, R. L. Walsworth, S. Hong, P. Maletinsky, and A. Yacoby, Nat. Nanotechnol. **9**, 279 (2014).
[14] A. O. Sushkov, I. Lovchinsky, N. Chisholm, R. L. Walsworth, H. Park, and M. D. Lukin, Phys. Rev. Lett. **113**, 197601 (2014).
[15] A. Abragam, *Principles of Nuclear Magnetism* (Oxford University Press, London, 1961).
[16] C. P. Slichter, *Principles of Magnetic Resonance* (Springer, Berlin, 1990).
[17] R. Kimmich, *NMR: Tomography, Diffusometry, Relaxometry* (Springer, Berlin, 1997).
[18] L. M. Norris, G. A. Paz-Silva, and L. Viola, Phys. Rev. Lett. **116**, 150503 (2016).
[19] L. Viola and S. Lloyd, Phys. Rev. A **58**, 2733 (1998).
[20] L. Viola, E. Knill, and S. Lloyd, Phys. Rev. Lett. **82**, 2417 (1999).
[21] P. Zanardi, Phys. Lett. A **258**, 77 (1999).
[22] K. Khodjasteh and D. A. Lidar, Phys. Rev. Lett. **95**, 180501 (2005).
[23] G. S. Uhrig, Phys. Rev. Lett. **98**, 100504 (2007).
[24] A. G. Kofman and G. Kurizki, Phys. Rev. Lett. **93**, 130406 (2004).
[25] A. G. Kofman and G. Kurizki, IEEE Trans. Nanotechnol. **4**, 116 (2005).
[26] A. G. Kofman and G. Kurizki, Phys. Rev. Lett. **87**, 270405 (2001).
[27] J. Clausen, G. Bensky, and G. Kurizki, Phys. Rev. Lett. **104**, 040401 (2010).
[28] G. Gordon, N. Erez, and G. Kurizki, J. Phys. B: At. Mol. Opt. Phys. **40**, S75 (2007).
[29] G. Gordon, G. Kurizki, and D. A. Lidar, Phys. Rev. Lett. **101**, 010403 (2008).
[30] G. Kurizki and A. Zwick, in *Advances in Chemical Physics, Vol. 159*, edited by P. Brumer, S. A. Rice, and A. R. Dinner, (John Wiley, New York, 2015).
[31] J. Clausen, G. Bensky, and G. Kurizki, Phys. Rev. A **85**, 052105 (2012).
[32] G. Gordon and G. Kurizki, Phys. Rev. Lett. **97**, 110503 (2006).
[33] G. Gordon and G. Kurizki, New J. Phys. **10**, 045005 (2008).
[34] H. Uys, M. J. Biercuk, and J. J. Bollinger, Phys. Rev. Lett. **103**, 040501 (2009).
[35] K. Khodjasteh, D. A. Lidar, and L. Viola, Phys. Rev. Lett. **104**, 090501 (2010).
[36] A. Ajoy, G. A. Álvarez, and D. Suter, Phys. Rev. A **83**, 032303 (2011).

[37] A. Zwick, G. A. Álvarez, G. Bensky, and G. Kurizki, New J. Phys. **16**, 065021 (2014).
[38] B. M. Escher, G. Bensky, J. Clausen, and G. Kurizki, J. Phys. B: At. Mol. Opt. Phys. **44**, 154015 (2011).
[39] D. Petrosyan, G. Bensky, G. Kurizki, I. Mazets, J. Majer, and J. Schmiedmayer, Phys. Rev. A **79**, 040304 (2009).
[40] G. Bensky, D. Petrosyan, J. Majer, J. Schmiedmayer, and G. Kurizki, Phys. Rev. A **86**, 012310 (2012).
[41] A. Zwick, G. A. Álvarez, and G. Kurizki, Phys. Rev. Appl. **5**, 014007 (2016).
[42] N. Shemesh, G. A. Álvarez, and L. Frydman, J. Magn. Res. **237**, 49 (2013).
[43] N. Shemesh, G. A. Álvarez, and L. Frydman, PLOS ONE **10**, e0133201 (2015).
[44] A. Feintuch, A. Grayevsky, N. Kaplan, and E. Dormann, Phys. Rev. Lett. **92**, 156803 (2004).
[45] D. Suter and R. R. Ernst, Phys. Rev. B **32**, 5608 (1985).
[46] G. A. Álvarez, D. Suter, and R. Kaiser, Science **349**, 846 (2015).
[47] G. A. Álvarez, R. Kaiser, and D. Suter, Ann. Phys. (NY) **525**, 833 (2013).
[48] P. Haikka, J. Goold, S. McEndoo, F. Plastina, and S. Maniscalco, Phys. Rev. A **85**, 060101 (2012).
[49] M. Gessner, M. Ramm, H. Haeffner, A. Buchleitner, and H.-P. Breuer, Europhys. Lett. **107**, 40005 (2014).
[50] A. Smirne, S. Cialdi, G. Anelli, M. G. A. Paris, and B. Vacchini, Phys. Rev. A **88**, 012108 (2013).
[51] E.-M. Laine, H.-P. Breuer, J. Piilo, C.-F. Li, and G.-C. Guo, Phys. Rev. Lett. **108**, 210402 (2012).
[52] B.-H. Liu, D.-Y. Cao, Y.-F. Huang, C.-F. Li, G.-C. Guo, E.-M. Laine, H.-P. Breuer, and J. Piilo, Sci. Rep. **3**, 1781 (2013).
[53] S. Wissmann and H.-P. Breuer, Phys. Rev. A **90**, 032117 (2014).
[54] A. Rivas, S. F. Huelga, and M. B. Plenio, Rep. Prog. Phys. **77**, 094001 (2014).
[55] H.-P. Breuer, E.-M. Laine, J. Piilo, and B. Vacchini, Rev. Mod. Phys. **88**, 021002 (2016).
[56] S. L. Braunstein and C. M. Caves, Phys. Rev. Lett. **72**, 3439 (1994).
[57] M. G. A. Paris, Int. J. Quantum Inf. **07**, 125 (2009).
[58] B. M. Escher, R. L. de Matos Filho, and L. Davidovich, Nat. Phys. **7**, 406 (2011).
[59] C. Benedetti and M. G. Paris, Phys. Lett. A **378**, 2495 (2014).
[60] M. A. C. Rossi and M. G. A. Paris, Phys. Rev. A **92**, 010302 (2015).
[61] N. Bar-Gill, L. M. Pham, C. Belthangady, D. L. Sage, P. Cappellaro, J. R. Maze, M. D. Lukin, A. Yacoby, and R. Walsworth, Nat. Commun. **3**, 858 (2012).
[62] J. Medford, L. Cywiński, C. Barthel, C. M. Marcus, M. P. Hanson, and A. C. Gossard, Phys. Rev. Lett. **108**, 086802 (2012).
[63] Y. Romach, C. Müller, T. Unden, L. J. Rogers, T. Isoda, K. M. Itoh, M. Markham, A. Stacey, J. Meijer, S. Pezzagna, B. Naydenov, L. P. McGuinness, N. Bar-Gill, and F. Jelezko, Phys. Rev. Lett. **114**, 017601 (2015).
[64] G. De Lange, Z. Wang, D. Riste, V. Dobrovitski, and R. Hanson, Science **330**, 60 (2010).
[65] A. Kofman, G. Kurizki, and B. Sherman, J. Mod. Opt. **41**, 353 (1994).
[66] D. Gelbwaser-Klimovsky, R. Alicki, and G. Kurizki, Phys. Rev. E **87**, 012140 (2013).
[67] H. Y. Carr and E. M. Purcell, Phys. Rev. **94**, 630 (1954).
[68] S. Meiboom and D. Gill, Rev. Sci. Instrum. **29**, 688 (1958).
[69] G. Kurizki, E. Shahmoon, and A. Zwick, Phys. Scr. **90**, 128002 (2015).
[70] H. Cramér, *Mathematical Methods of Statistics* (Princeton University Press, Princeton, 1946).
[71] G. A. Álvarez, E. P. Danieli, P. R. Levstein, and H. M. Pastawski, J. Chem. Phys. **124**, 194507 (2006).
[72] E. Danieli, G. Álvarez, P. Levstein, and H. Pastawski, Solid State Commun. **141**, 422 (2007).
[73] I. Rotter, J. Phys. A: Math. Theor. **42**, 153001 (2009).
[74] J. P. Garrahan and I. Lesanovsky, Phys. Rev. Lett. **104**, 160601 (2010).
[75] I. Lesanovsky, M. van Horssen, M. Gutua, and J. P. Garrahan, Phys. Rev. Lett. **110**, 150401 (2013).
[76] I. Rotter and J. P. Bird, Rep. Prog. Phys. **78**, 114001 (2015).
[77] C. O. Bretschneider, G. A. Álvarez, G. Kurizki, and L. Frydman, Phys. Rev. Lett. **108**, 140403 (2012).
[78] J. Stepisnik, Physica B **183**, 343 (1993).
[79] H.-P. Breuer and F. Petruccione, *The Theory of Open Quantum Systems* (Oxford University Press, Oxford, 2007).
[80] G. Gordon, J. Phys. B: At. Mol. Opt. Phys. **42**, 223001 (2009).
[81] C. Benedetti, F. Buscemi, P. Bordone, and M. G. A. Paris, Phys. Rev. A **89**, 032114 (2014)